



## Crosslink-enhanced strategy to achieve multicolor long-lived room temperature phosphorescent films with excellent photostability

Taotao Li, Yu Zheng, Chenqin Wu, Chengyu Yan, Cheng Zhang\*, Hong Gao, Qian Chen, Kui Zhang\*

School of Chemistry and Chemical Engineering, Anhui University of Technology, Ma'anshan 243032, China

### ARTICLE INFO

#### Article history:

Received 19 October 2021

Revised 8 March 2022

Accepted 9 March 2022

Available online 13 March 2022

#### Keywords:

Crosslink

Film

Phosphorescence

Photostability

Multicolor

### ABSTRACT

Room temperature phosphorescence (RTP) films have recently attracted increasing attention due to their excellent luminescent properties for information encryption, optoelectronic devices, and sensors. However, polyvinyl alcohol (PVA) films with abundant hydrogen bonds to suppress triplet energy dissipation suffered from the humidity induced phosphorescence quenching under storage in the air for a long time. In this work, poly(acrylic acid) (PAA) was selected to crosslink PVA matrix through esterification reactions for preparing water resistant RTP films. The blue, cyan, and orange emissive RTP films were successfully obtained by incorporating three different organic compounds into PVA-PAA crosslinking films. Crosslinking strategy significantly improved the phosphorescence emissions of the doped films, and effectively blocked the absorption of water molecular, leading to the excellent photostability of the developed films. As a proof of concept, the white light phosphorescence film and anti-counterfeiting applications were successfully demonstrated.

© 2022 Published by Elsevier B.V. on behalf of Chinese Chemical Society and Institute of Materia Medica, Chinese Academy of Medical Sciences.

Luminescent films as smart solid-state materials have attracted broad research interests due to their diverse applications in optoelectronic devices, information storage, anti-counterfeiting, and sensors [1–5]. The luminescent films can be easily achieved by introducing phosphors into host matrices [6–9]. In this case, the luminophore can be immobilized into the film by covalent linkage, hydrogen bond interactions, and others. Depending on the nature of the doped phosphors, the films can produce different forms of luminescence such as fluorescence, phosphorescence, upconversion luminescence [10–12].

Long-lived room temperature phosphorescent (RTP) materials exhibit unique optical properties and essential applications due to their sustained luminescence after removing the excitation light source [13–17]. However, achieving long-lived RTP remains a significant challenge because of weak intersystem crossing (ISC), incidental non-radiative transitions, and undesirable molecular vibrations/rotations. Some strategies, such as crystallization engineering, H-aggregation, and construction of metal-organic framework, were adopted to obtain long-lived RTP [18–21], but suffering from the difficulties of processability, high cost, and metal toxicity. To overcome these problems, various film matrices with excellent prop-

erties were designed to enhance RTP. For example, bright RTP can be obtained with a quantum yield of 7.5% by doping small molecules in poly(methyl methacrylate) (PMMA) through directed halogen bonding that vibrational dissipation of triplet excitons can be effectively suppressed [22]. Recently, nacre-inspired nanocomposite with controlled RTP retention time was achieved through introducing waterborne RTP polymers into the self-assembled polymer/nanoclay films [23]. The nanocomposite films possess outstanding mechanical properties and processability, and can achieve oxygen permeation and diffusion inside by adjusting the ratio of polymeric nanoclays. Unfortunately, the specific film matrix has disadvantages of complicated design and operation, which cannot be used as a universal film matrix for obtaining RTP.

Polyvinyl alcohol (PVA) has been widely used as film-former material due to its good hydrophilicity, optical transparency, and flexible processability [24–26]. Su *et al.* completed excitation-dependent ultralong organic luminescence (UOL) via doping various pyrene derivatives into the host PVA matrix while controlling the aggregation state of the luminescent molecules and hydrogen bonds formation to extend the color of the afterglow to the red range [27]. PVA contains many hydroxyl groups to construct tight hydrogen bond networks, but it is susceptible to absorb water and damp leading to the destruction of hydrogen bonding interactions and phosphorescence quenching. In this work, we developed a novel crosslink-enhanced strategy to achieve multicolor

\* Corresponding authors.

E-mail addresses: [c Zhang@ahut.edu.cn](mailto:c Zhang@ahut.edu.cn) (C. Zhang), [zhangkui@mail.ustc.edu.cn](mailto:zhangkui@mail.ustc.edu.cn) (K. Zhang).

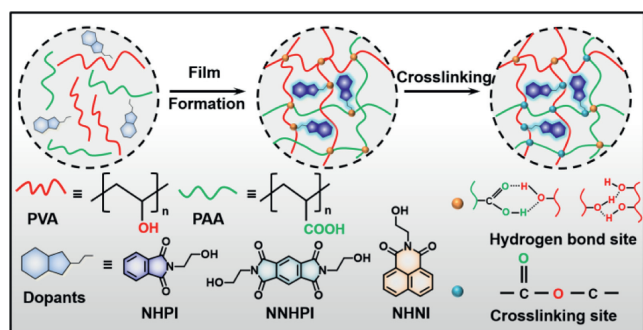


**Fig. 1.** Schematic illustration of the fabricating processes of PVA-PAA crosslinking phosphorescent film and the chemical structures of NHPI, NNHPI and NHNI.

long-lived phosphorescent films with excellent photostability. PVA was selected as film matrix, which was crosslinked by poly(acrylic acid) (PAA) under thermal treatment. The multicolor emissive RTP polymer films were successfully obtained by incorporating different organic molecules into PVA-PAA crosslinking films. Esterification crosslinking occurred between the carboxyl group of PAA and the hydroxyl group of PVA formed stable chemical bonds to suppress the dissipation of triplet excitons. Meanwhile, the crosslinking strategy significantly improved the water resistance properties of the PVA-based phosphorescent films. In addition, the obtained crosslinking films have not only reliable water resistance to guarantee phosphorescent emission, but also excellent optical transparency and processability properties, providing potential applications in many fields.

The PVA-PAA films were prepared by blending different mass ratios of PVA:PAA in solution (Table S1 in Supporting information) and drying in a hot oven for 3 h at 70 °C. Thereafter, the crosslinked film was fabricated by thermal treatment at 150 °C for 1 h through an esterification reaction. The obtained films were colorless and transparent with excellent transmittance in the range of 400–700 nm (Fig. S1 in Supporting information). To verify that the PVA-PAA crosslinking film was suitable as RTP matrix, three different organic compounds *N*-(2-hydroxyethyl)phthalimide, *N,N'*-(2-hydroxyethyl)pyromellitimide, and *N*-(2-hydroxyethyl)-1,8-naphthalimide, named NHPI, NNHPI, and NHNI (Fig. 1 and Figs. S2–S4 in Supporting information) were selected and doped into the films to achieve long-lived RTP. The three organic compounds have different degree of conjugation, indicating that they could display various colors of RTP emission [28].

Detailed experiments were carried out to investigate the RTP emissions of three organic compounds in crosslinking films. Three-dimensional (3D) phosphorescent spectra of the doped PVA-30%PAA crosslinking films illustrated the main emission centers of NHPI and NNHPI are 450 and 480 nm, respectively, when the excitation wavelength varied from 200 nm to 360 nm (Figs. 2a and b). The main emission centers of NHNI doped film were 545 and 580 nm, when the excitation wavelength varied from 200 nm to 400 nm (Fig. 2c). The emission peaks of the three films showed excitation-independence, which can be proved from the phosphorescence spectra under different excitation wavelengths in Fig. S5 (Supporting information). Interestingly, NHPI, NNHPI, and NHNI doped PVA-PAA crosslinking films exhibited noticeable phosphorescence afterglow to the naked eyes (~1.5 s) under ambient conditions when the UV light source was turned off. Due to the different emission centers of the three films, they exhibit the corresponding phosphorescent colors: blue for NHPI (Fig. 2d), cyan for NNHPI (Fig. 2e), and orange for NHNI (Fig. 2f), respectively. The corresponding Commission International de l'Eclairage (CIE) coordinates were (0.15, 0.14), (0.17, 0.32), and (0.44, 0.54), respectively (Fig. S6 in Supporting information). The quantum yields (QYs) of

the three films can reach 21.55%, 10.24% and 18.26%, respectively. All of the doped films were transparent under daylight (Fig. S7 in Supporting information), and the phosphorescence lifetimes were 527.67, 392.54, and 365.20 ms, respectively (Fig. S8 and Table S2 in Supporting information), which were higher than reported RTP films (Table S3 in Supporting information).

To further reveal this interesting long-lived RTP phenomenon in PVA-PAA crosslinking film, we performed the phosphorescence spectra of the three compounds as solid powder (Fig. S9 in Supporting information) or in ethanol solution (Fig. S10 in Supporting information). Solid powders and ethanol solutions of these compounds were all without phosphorescent emission. However, strong phosphorescence emerged when the three organic molecules were doped into the PVA-PAA crosslinking films, indicating that the crosslinking films significantly inhibited the non-radiative transition process and improved phosphorescence emission. Previous reports have indicated that doping concentrations in the film could influence luminescence behavior [26]. Hence, different doping concentrations in the films were systematically investigated. NHPI, NNHPI, and NHNI with the different mass fraction in the PVA-30%PAA films (0.05%, 0.1%, 0.5%, 1%, 2%, and 5%) are prepared (Table S4 in Supporting information). As shown in Fig. S11 (Supporting information), the three phosphorescent films at low concentrations can lead to phosphorescent emission. The three compounds are dispersed in the film with molecular state, which can be supported by the UV-vis absorption spectra (Fig. S12 in Supporting information). The maximum absorption peaks of NHPI, NNHPI, and NHNI in ethanol solution were identical with the peaks in PVA-30%PAA films (0.5% doped), but not coincide with solid powder. Unfortunately, the high doping concentrations (more than 0.5%) caused the decline of phosphorescence intensity in NHPI and NNHPI doped films, which could be attributed to aggregation caused quenching effect (Figs. S13a and b in Supporting information). For NHNI doped films, high doping concentrations (more than 1%) induced precipitation of dopants in the film, which can be explained by the poor solubility of NHNI in water (Fig. S13c in Supporting information). Therefore, the weight fraction of 0.5% is the most suitable doping concentration for PVA-PAA film to accomplish long-lived phosphorescent emission under ambient conditions.

We also study the PAA content that affects the phosphorescence performance, the 0.5% NHPI doped PVA-PAA crosslinking films with PAA composition of 0, 10, 20, 30, 40, and 50 wt% were synthesized (Table S5 in Supporting information). As shown in Fig. 3a, with increasing PAA content, the phosphorescent emission intensity of NHPI doped crosslinking films enhanced remarkably. Compared with doping in pure PVA films, the phosphorescence intensities of NHPI, NNHPI, and NHNI doped in PVA-30%PAA crosslinking films were increased by 16.23, 9.54, and 1.86 times, respectively (Fig. S14a in Supporting information). More attractively, the lifetimes were increased by 4.67, 2.87, and 1.38 times for NHPI, NNHPI, and NHNI doped crosslinking films when 30% PAA was used (Fig. S14b and Table S6 in Supporting information). The possible mechanism can be attributed to the crosslinking esterification reaction between PVA and PAA through heat-treatment.

To verify the crosslinking process, PVA-PAA films were characterized by FT-IR spectroscopy, X-ray diffraction measurement (XRD), and thermogravimetric analysis (TGA). Fig. 3b showed the FT-IR spectra of the pure PVA film and various ratios of crosslinking films. The broad and strong peak at 3340  $\text{cm}^{-1}$  could be attributed to the stretching vibration of the O–H bond. The peak at 2920  $\text{cm}^{-1}$  was caused by the stretching vibration of C–H in the  $-\text{CH}_2$  functional group. A new peak appeared at 1710  $\text{cm}^{-1}$  when PAA was continuously added in the film, which originated from the stretching vibration of C=O functional group. It is important to note that the stretching vibration of C–O bond at 1240  $\text{cm}^{-1}$

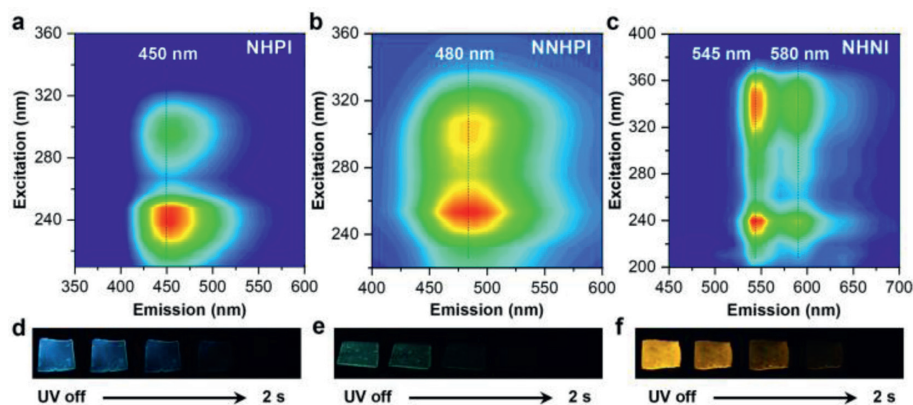


**Fig. 2.** Optical properties of phosphorescent PVA-PAA crosslinking film. 3D phosphorescence spectra of (a) NHPI, (b) NNHPI, and (c) NHNI doped PVA-30%PAA crosslinking films. The photographs of the (d) NHPI, (e) NNHPI, and (f) NHNI doped PVA-30%PAA crosslinking films taken after ceasing 254 nm irradiation.

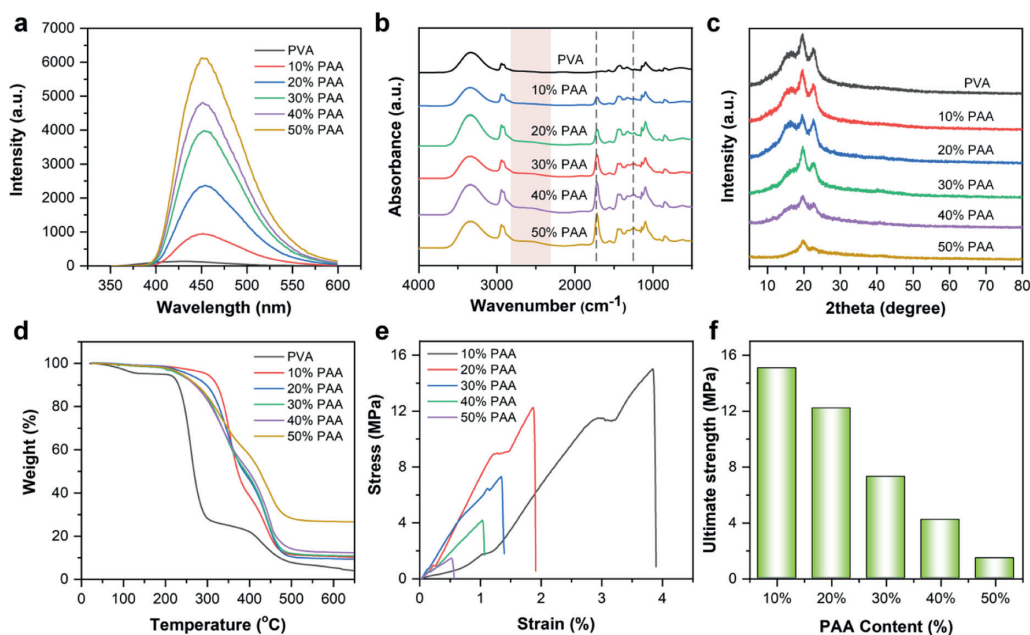


**Fig. 3.** (a) Phosphorescence spectra of PVA-PAA crosslinking films (doped with 0.5% of NHPI) with different PAA content; (b) FT-IR spectra, (c) XRD patterns, (d) TGA curves, (e) stress-strain curves of PVA-PAA crosslinking films with different PAA content; (f) the ultimate strength of PVA-PAA crosslinking films with different PAA content.

effectively strengthened by esterification crosslinking between hydroxyl and carboxyl groups [29]. Moreover, a wide range of absorption from  $2800\text{ cm}^{-1}$  to  $2400\text{ cm}^{-1}$  indicated the intermolecular and intramolecular hydrogen bonds in the crosslinking films. The XRD was conducted to measure the crystallinity of PVA-PAA crosslinking film. Fig. 3c described the semi-crystalline for pure PVA films with diffraction peaks at  $16.1^\circ$ ,  $19.8^\circ$ , and  $22.8^\circ$ . However, the intensity dramatically decreased with increasing PAA content, illustrating that the amorphous region became dominant [30]. The crystalline peak was very weak as the composition of PAA reached 50 wt%, and the amorphous film can be further indicated the esterification crosslinking between PAA and PVA. The thermal stability of the developed PVA-PAA crosslinking film was determined using TGA (Fig. 3d). The weight loss with  $\sim 5\%$  of pure PVA film below  $250^\circ\text{C}$  was related to the loss of low molecular weight compounds (typically absorbed water). However, for PVA-PAA crosslinking films, the weight loss is negligible at this stage, illustrating the elimination of water quencher by heat-treatment and crosslinking. In the range of  $250\text{--}350^\circ\text{C}$ , the weight loss could be explained by the decomposition of the uncrosslinked carboxyl groups in the films [31]. Further increasing the temperature

( $>350^\circ\text{C}$ ) resulted in the breakage of the polymer chains in the films. These results confirmed the esterification crosslinking between PAA and PVA, and proved that the crosslinking films exhibited higher thermal stability than pure PVA film.

Although increasing the proportion of PAA can improve the phosphorescent properties of the film, the high crosslinking level leads to a decline in mechanical properties. Fig. 3e displayed the tensile stress-strain curves of crosslinking films. The crosslinking impeded the movement between polymer chain segments, leading to a reduction in maximum strain. More importantly, the ultimate strength of the films decreased with increasing the percentage of PAA (Fig. 3f). That is to say, we have to balance the phosphorescent emission and mechanical properties of the film according to the specific conditions of use. In this work, the PVA:PAA mass ratio of 7:3 was selected to fabricate of crosslinking films to ensure excellent luminescence and mechanical performance.

Using PAA to crosslink the PVA also significantly improved the photostability of the phosphorescent films. Traditional RTP films using a single component of PVA as matrix absorbed moisture from the air, breaking intermolecular hydrogen bonds and causing a dramatic decline in the phosphorescent signal. To verify the

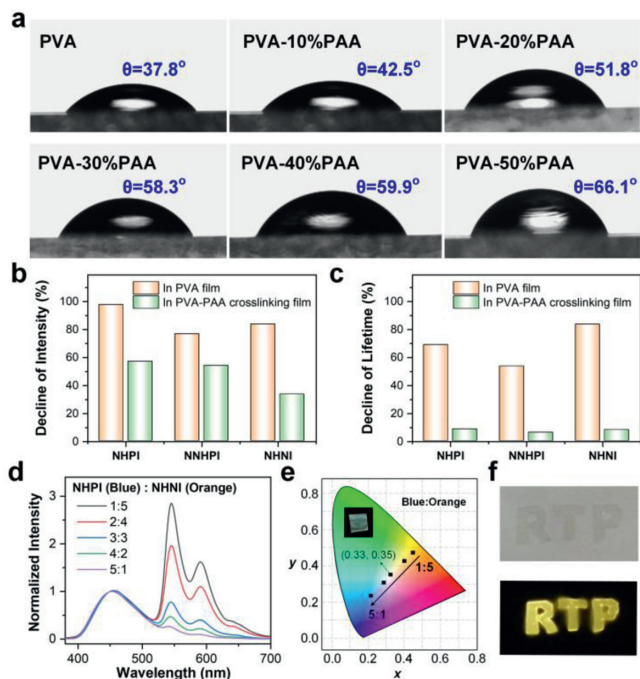


**Fig. 4.** (a) Water contact angle of PVA-PAA crosslinking films and pure PVA film; (b) the decline of phosphorescence intensity of 0.5% doped NHPI, NNHPI, and NHNI in pure PVA films and PVA-30%PAA crosslinking films after seven days of storage; (c) the decline of phosphorescence lifetime of 0.5% doped NHPI, NNHPI, and NHNI in pure PVA films and PVA-30%PAA crosslinking films after seven days of storage; (d) normalized phosphorescence spectra of different ratios of NHPI and NHNI co-doped PVA-30%PAA crosslinking films ( $\lambda_{\text{ex}} = 240 \text{ nm}$ ); (e) the CIE coordinate diagram of NHPI-NHNI films in accordance with (d); (f) the photographs of NHNI doped PVA-30%PAA crosslinking films with designed shapes.

moisture resistance, we first tested the water contact angle (WCA) of PVA-PAA crosslinking films. As shown in Fig. 4a, the WCA increased gradually from  $37.8^\circ$  to  $66.1^\circ$  with the increment of PAA content from 0 to 50 wt%. Compared with the pure PVA film, the PVA-PAA crosslinking films exhibited relatively weak hydrophilicity. Besides, we performed the water absorption test to investigate the moisture absorption performance of PVA-PAA crosslinking films and pure PVA film. The water absorption capacity is defined as the increment in relative weight before and after 24 h exposure to a humid environment (RH: 85%~90%). Table S7 (Supporting information) revealed the water absorption capacity decreased with adding PAA in the crosslinking films. These results further confirmed the water resistance by esterification in the crosslinking films [32].

Thanks to excellent resistance to moisture, the crosslinking films exhibited outstanding photostability under ambient conditions. The as-prepared NHPI, NNHPI, and NHNI doped PVA-30%PAA crosslinking films were stored at room temperature (RH: 50%~60%) for seven days, and the spectral characteristics were measured. As a comparison, three compounds doped pure PVA films were surveyed under identical conditions. As shown in Fig. 4b, the phosphorescence intensity of doped pure PVA films decreased severely compared to crosslinking films. More fascinatingly, the phosphorescence lifetimes of PVA-30%PAA crosslinking films only exhibited slight decline (8.6% for NHPI, 6.1% for NNHPI, 8.1% for NHNI doped films). On the contrary, the phosphorescence lifetimes of doped pure PVA films quenched sharply after seven days of storage (Fig. 4c). Such results strongly confirmed that the crosslinking films could prevent the destruction of hydrogen bonds by water molecules and phosphorescence quenching by oxygen in the air, providing great convenience for practical applications.

To demonstrate the universality of our proposed crosslinking enhancement strategy, several hydroxyl-free phosphors (including phthalimide, *N*-(2-bromoethyl)phthalimide, pyromellitic diimide, 1,8-naphthalimide, and 1,8-naphthalic acid) were selected to dope into PVA-30%PAA crosslinking films and pure PVA films by using same method. Spectral results showed that all these organic molecules without hydroxyl groups in the crosslinking films have significantly enhanced phosphorescence lifetimes than that in PVA films (Table S8 in Supporting information). In addition, carbon dots (CDs), as a common nanomaterial to achieve RTP, were also adopted to prove the versatility of crosslinking films. N/P-doped CDs and nitrogen heterocyclic functionalized CDs in crosslinking films displayed a remarkable improvement in phosphorescence lifetime over that in pure PVA films (Table S9 in Supporting information), which indicated that PAA crosslinked with PVA can improve the performance of PVA as single matrix to realize RTP emission.

Benefiting from the high transparency, good stability, and excellent luminescent performance, NHPI (blue emission) and NHNI (orange emission) were co-doped with various mass ratios in 30 wt% PAA crosslinking films to prepare white light emission film (Table S10 in Supporting information). Phosphorescence spectra in Fig. 4d showed the emission peaks at 450, 545, and 580 nm of the dual-doping crosslinking films. Because of the low doping concentration, the simultaneous doping of the NHPI and NHNI did not affect their inherent luminescence. At a specific ratio of NHPI (0.3 wt%):NHNI (0.3 wt%), white light emission with the Commission International de l'Éclairage (CIE) coordinates of (0.33, 0.35) can be obtained (Fig. 4e). Furthermore, the films can be cut to the desired shapes due to the advantage of good reprocessability. As shown in Fig. 4f, the 0.5 wt% NHNI doped PVA-30%PAA crosslinking film was carved into the letters of "RTP", and the distinctive yellow phosphorescence could be observed by the naked eye when the UV excitation light was turned off. These outstanding optical properties make them potentially apply in information storage and anti-counterfeiting.

In summary, we have demonstrated a promising strategy to obtain long-lived RTP films with high transparency, excellent luminescence, and outstanding humidity resistance. Our research revealed that the high temperature heat-treatment of crosslinking esterification reaction between PVA and PAA played an essential role in immobilizing dopants and protecting triplet excited states. By doping different dopants in the crosslinking films with reasonable concentrations, multicolor RTP emissions including white light can be easily achieved. In addition, crosslinking esterification endows humidity resistance of the developed films, thus the lifetime of crosslinking film exhibits high stability within seven days. The crosslinking films can be potential applied in the fields of anti-counterfeiting and chemical sensors.

#### Declaration of competing interest

The authors declare that there have no known competing financial interests or personal relationships that could have appeared to influence the work reported in this paper.

#### Acknowledgments

This work was supported by the National Natural Science Foundation of China (No. 22106005), Natural Science Foundation of Anhui Province (No. 1908085MB41), Natural Science Foundation of Anhui Province for Distinguished Young Scholars (No. 2008085J11), and Innovative Training Program for College Students (No. S202110360206).

## Supplementary materials

Supplementary material associated with this article can be found, in the online version, at doi:10.1016/j.ccl.2022.03.047.

## References

- [1] J. He, B. Ji, S. Koley, U. Banin, D. Avnir, *ACS Nano* 13 (2019) 10826–10834.
- [2] Y. Ma, L. Shen, P. She, et al., *Adv. Opt. Mater.* 7 (2019) 1801657.
- [3] R. Gao, M.S. Kodaimati, D. Yan, *Chem. Soc. Rev.* 50 (2021) 5564–5589.
- [4] Y. Ding, X. Wang, M. Tang, H. Qiu, *Adv. Sci.* 9 (2021) 2103833.
- [5] W. Guan, W. Zhou, J. Lu, C. Lu, *Chem. Soc. Rev.* 44 (2015) 6981–7009.
- [6] Z. Wang, T. Li, B. Ding, X. Ma, *Chin. Chem. Lett.* 31 (2020) 2929–2932.
- [7] M. Louis, H. Thomas, M. Gmelch, et al., *Adv. Mater.* 31 (2019) 1807887.
- [8] T. Han, H. Deng, Z. Qiu, et al., *J. Am. Chem. Soc.* 140 (2018) 5588–5598.
- [9] S. Shi, W. Bai, T. Xuan, et al., *Small Method* 5 (2020) 2000889.
- [10] G. Qu, Y. Zhang, X. Ma, *Chin. Chem. Lett.* 30 (2019) 1809–1814.
- [11] K. Jiang, S. Sun, L. Zhang, et al., *Angew. Chem. Int. Ed.* 54 (2015) 5360–5363.
- [12] Y. Zhou, W. Qin, C. Du, et al., *Angew. Chem. Int. Ed.* 58 (2019) 12102–12106.
- [13] T. Zhang, X. Ma, H. Wu, et al., *Angew. Chem. Int. Ed.* 59 (2020) 11206–11216.
- [14] Y. Sun, X. Zhang, J. Zhuang, et al., *Carbon* 165 (2020) 306–316.
- [15] Y. Yang, X. Fang, S.S. Zhao, et al., *Chem. Commun.* 56 (2020) 5267–5270.
- [16] C. Wang, T. Jiang, X. Ma, *Chin. Chem. Lett.* 31 (2020) 2921–2924.
- [17] G. Wang, Z. Wang, B. Ding, X. Ma, *Chin. Chem. Lett.* 32 (2021) 3039–3042.
- [18] Y. Yang, K.Z. Wang, D. Yan, *Chem. Commun.* 53 (2017) 7752–7755.
- [19] B. Zhou, D. Yan, *Angew. Chem. Int. Ed.* 58 (2019) 15128–15135.
- [20] B. Zhou, D. Yan, *Sci. China Chem.* 64 (2021) 509–510.
- [21] G. Xiao, B. Zhou, X. Fang, D. Yan, *Research* 2021 (2021) 9862327.
- [22] D. Lee, O. Bolton, B.C. Kim, et al., *J. Am. Chem. Soc.* 135 (2013) 6325–6329.
- [23] X. Yao, J. Wang, D. Jiao, et al., *Adv. Mater.* 33 (2021) 2005973.
- [24] R. Gao, X. Fang, D. Yan, *J. Mater. Chem. C* 6 (2018) 4444–4449.
- [25] Y. Zhang, Y. Su, H. Wu, et al., *J. Am. Chem. Soc.* 143 (2021) 13675–13685.
- [26] H. Wu, L. Gu, G.V. Baryshnikov, et al., *ACS Appl. Mater. Interfaces* 12 (2020) 20765–20774.
- [27] Y. Su, Y. Zhang, Z. Wang, et al., *Angew. Chem. Int. Ed.* 59 (2020) 9967–9971.
- [28] L. Gu, H. Wu, H. Ma, et al., *Nat. Commun.* 11 (2020) 944–948.
- [29] J.W. Rhim, M.Y. Sohn, H.J. Joo, K.H. Lee, *J. Appl. Polym. Sci.* 50 (1993) 679–684.
- [30] M. Lim, H. Kwon, D. Kim, et al., *Prog. Org. Coat.* 85 (2015) 68–75.
- [31] R. Liang, H. Yuan, G. Xi, Q. Zhou, *Carbohydr. Polym.* 77 (2009) 181–187.
- [32] M. Lim, D. Kim, J. Seo, *Polym. Int.* 65 (2016) 400–406.